



Erzgraber, H., Wille, E., Krauskopf, B., & Fischer, I. (2008). *Amplitude-phase dynamics near the locking region of two delay-coupled semiconductor lasers*. <http://hdl.handle.net/1983/1181>

Early version, also known as pre-print

[Link to publication record in Explore Bristol Research](#)  
PDF-document

## University of Bristol - Explore Bristol Research

### General rights

This document is made available in accordance with publisher policies. Please cite only the published version using the reference above. Full terms of use are available:  
<http://www.bristol.ac.uk/red/research-policy/pure/user-guides/ebr-terms/>

# Amplitude-phase dynamics near the locking region of two delay-coupled semiconductor lasers

H. Erzgräber<sup>1</sup>, E. Wille<sup>2</sup>, B. Krauskopf<sup>3</sup>, and I. Fischer<sup>4</sup>

<sup>1</sup>School of Engineering, Computing and Mathematics, University of Exeter, Exeter EX4 4QF, United Kingdom

<sup>2</sup>Institute of Applied Physics, Darmstadt University of Technology, Schloßgartenstraße 7, 64289 Darmstadt, Germany

<sup>3</sup>Department of Engineering Mathematics, University of Bristol, Bristol BS8 1TR, United Kingdom

<sup>4</sup>Joint Research Institute for Integrated Systems and School of Engineering and Physical Sciences, Heriot-Watt University, Edinburgh EH14 4AS, Scotland, United Kingdom

E-mail: [h.erzgraber@exeter.ac.uk](mailto:h.erzgraber@exeter.ac.uk)

**Abstract.** We investigate the dynamical properties of two mutually delay-coupled semiconductor lasers that are coupled via their optical fields. Because a semiconductor laser is an oscillator that features strong coupling between its amplitude and phase, this system serves as a prototype model of coupled amplitude-phase oscillators. Our main interest here is in the dynamics near and within the locking region where the two lasers emit light of the same frequency. We present experimental observations that give evidence for four qualitatively different dynamical regimes: stable continuous wave emission, oscillations at the laser's characteristic relaxation oscillation frequency, oscillation related to the frequency difference between the two lasers, and chaotic dynamics. We characterise and identify these dynamical regimes and analyse them by means of a bifurcation analysis of the corresponding rate equation model with delay. Specifically, we present the underlying bifurcation structure, where the detuning and the pump current are the main bifurcation parameter. The combination of experiment and bifurcation analysis shows how changes of the dynamics arise from the presence of local and global bifurcations near the locking region.

PACS numbers: 42.65.Sf, 05.45.Xt, 02.30.Ks, 42.55.Px

Keywords: *coupled semiconductor lasers, delay-instabilities, bifurcation analysis*: Article preparation, IOP journals Submitted to: *Nonlinearity*

## 1. Introduction

Coupled nonlinear oscillators can be found in many scientific disciplines, including physics, chemistry, biology and engineering, and it is now well established that they may exhibit rich and complex dynamical behaviour [1, 19, 37, 50]. An issue that has been acknowledged only quite recently is the fact that the ensuing dynamics of the system may be affected in an important way by the presence of sufficiently large time-delay in the coupling. Several dynamical effects have been attributed to delay, such as the suppression of coupled oscillations and partial locking or synchronisation; see, for example, [3, 5, 6, 47, 29, 41, 45, 48, 49, 56]. Nevertheless, there are still many challenges when it comes to a global understanding of the basic dynamical regimes displayed by delay-coupled systems.

Mutually-coupled semiconductor lasers are an attractive class for the study of delay-induced instabilities for a number of reasons. First of all, semiconductor lasers are quite robust and accessible experimentally, and the delay arises naturally due to the travel time of light (or electronic signals in some schemes) between optical components. The intrinsic time scales are on the order of pico- to nano-seconds, so that even short distances between optical elements result in considerable delay times. Furthermore, due to the often low reflectivities of their facet mirrors, semiconductor lasers are very susceptible to external light injection. Delayed-feedback and delay-coupled semiconductor lasers are not only of interest from a fundamental point of view, but they also play an important role in technological applications — most importantly in optical data storage or optical data transmission. For these reasons, delay-induced dynamics in (semiconductor) laser systems have been studied since the early days after the invention of the lasers. The original interest has been in the effect of reflections back into the laser [4, 13, 14, 15, 34, 35, 36, 38, 42, 44, 46], but more recently there has been a focus on different types of delay-coupled lasers; see, for example, Refs. [2, 7, 16, 17, 23, 25, 26, 27, 40, 43, 52, 53, 55].

From the modelling point of view, semiconductor laser systems can often be described in very good agreement with experiments via rate equation models, which are simple enough to allow for comprehensive bifurcation studies in many cases [28, 32, 54]. Importantly, semiconductor lasers are general nonlinear oscillators with the particularity that they feature a strong coupling between amplitude and phase of the optical field [24]. Thus, a reduction to simpler amplitude equations or phase-oscillator models is possible only under particular circumstances. In general, both the amplitude and the phase of the coupling field have to be taken into account [12]; this is also known from semiconductor lasers with optical feedback [21, 22]. In the specific case of delay-coupling between lasers, an extra difficulty is that the rate equation model takes the form of a delay differential equation (DDE) with an infinite dimensional phase space [8, 20]. However, in recent years advanced computational tools [9, 18, 31, 51] have become available for the bifurcation analysis of DDEs with several fixed delays. In fact, the wish to understand laser systems with delays has been one of the driving factors behind the development of

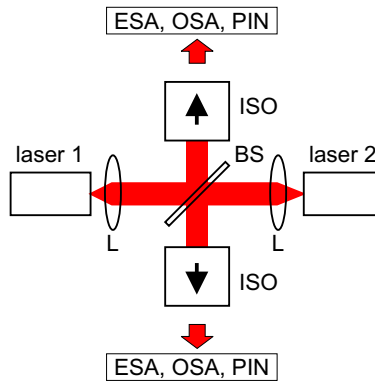


**Figure 1.** Experimental setup of two mutually delay-coupled lasers with collimating lenses (L), beamsplitter (BS), and optical isolators (ISO); the detection branches consist of an electrical spectrum analyser (ESA) with fast avalanche photo diodes (APD), and an optical spectrum analyser (OSA) with slow photo diodes (PIN).

these tools; see also [30].

In this paper we consider a system consisting of two similar semiconductor lasers that are mutually delay-coupled in a face-to-face configuration via their optical fields; see figure 1 for the experimental realisation. In previous studies we considered the role of compound laser modes (CLMs) for locking between the two lasers [12], the influence of the pump current [10] and the detuning (frequency difference) between the two lasers [11]. The dynamics outside the locking region was investigated in Ref. [55]. The focus here is on a comprehensive bifurcation analysis of the system near and within its locking region, guided by the experimental identification of different dynamical regimes. The measurements consist of recorded peaks of optical spectra and radio frequency (rf) spectra (also referred to as relative intensity noise (RIN) spectra) as a function of the detuning for three fixed levels of the pump current. Specifically, we show how the observed stable locking, relaxation oscillations, detuning oscillations and chaotic dynamics are organised by a bifurcation diagram in the two-dimensional parameter plane of detuning versus pump current. Transitions between different dynamical behaviour of the system are thus identified as the crossing of certain bifurcation curves. The bifurcation curves in turn divide the parameter plane into regions of stable CLMs, stable relaxation oscillations, and stable detuning oscillations; transitions to chaotic dynamics are also identified.

This paper is organised as follows. The delay-coupled laser system is described in section 2, both in terms of the experimental realisation as well as the rate equation model. In section 3 we present the experimental findings of the dynamical behaviour; the measurements are directly compared with numerical simulations of the rate equations (to demonstrate the accuracy of the latter). We proceed with a comprehensive bifurcation analysis of the locking region in section 4, identifying regions of stable CLMs, relaxation oscillations and the detuning oscillations. Finally, in section 5 we summarise our results, draw conclusion and point to future work.

## 2. Face-to-face coupled semiconductor lasers

The experimental setup consisting of two semiconductor lasers that receive part of each other's emitted light in a face-to-face configuration is sketched in figure 1. The lasers are single-mode distributed feedback (DFB) semiconductor lasers, which were hand selected to obtain two practically identical devices. Under uncoupled conditions, the nominal wavelength of each laser is 1540 nm, which corresponds to a frequency of about  $1.9 \times 10^{14}$  Hz, and their threshold currents (defining onset of laser operation) are 9.0 mA. Above the laser threshold the lasing fields of the lasers are larger than zero (the laser is 'on') and increasing the pump current further increases the amplitude of the optical field, resulting in increasing output power of the lasers. As most semiconductor lasers, the two lasers display characteristic damped relaxation oscillations when perturbed; the relaxation frequencies for both lasers were estimated experimentally to range from 0 to 10 GHz, for pump currents between 9 and 24 mA. The coupling between amplitude and phase of the optical field can be expressed by the linewidth-enhancement (or Henry) factor [24], which was determined experimentally as  $\alpha = 2$  for both lasers. The distance between the two lasers results in a time delay  $\tau = \frac{L}{c}$  in the coupling, where  $L$  is the optical path length from laser 1 to laser 2, and  $c$  is the speed of light. In our setup we choose  $L = 51 \pm 1$  mm, which results in a delay time of  $\tau = (170 \pm 3) \times 10^{-12}$  s, corresponding to a round-trip frequency of  $\nu_{ext} = 2.9 \pm 0.1$  GHz. The coupling between the lasers was estimated experimentally: approximately 5% of the output power of each laser entered into the respective other laser.

Due to the fast time scales of the intensity oscillations in semiconductor lasers, the dynamics is characterised via spectra. They are measured from two detection branches, which include optical isolators (ISO) to prevent unwanted feedback. Firstly, to identify the characteristics of the optical fields we measure optical spectra with an optical spectrum analyser (OSA). Secondly, we also measure radio frequency (rf) spectra of the laser intensities, by detecting the intensity fluctuations via two avalanche photo diodes (bandwidth 12 GHz) and then analysing them with an electrical spectrum analyser (ESA). The main bifurcation parameters in our studies are the (identical) pump currents of both lasers and the optical frequency  $\nu_2$  of laser 2. The optical frequency  $\nu_1$  of laser 1 is kept fixed. The optical frequency of a semiconductor laser can be detuned via small adjustments to the controlled temperature of the laser. Effects of the temperature change on other laser parameters can be neglected. Changing the optical frequency  $\nu_2$ , results in a relative detuning  $\Delta = \nu_2 - \nu_1$  between the lasers. We characterise the dynamics of the coupled laser system by recording the peaks of optical and rf spectra as a function of  $\Delta$  for different fixed values of the pump current. Note that such bifurcation diagrams are not symmetric around zero detuning, because of the asymmetrical change of the detuning  $\Delta$  via  $\nu_2$  which is experimentally most convenient. (A symmetrical change of  $\Delta$  would require a simultaneous change of  $\nu_1$  and  $\nu_2$  in opposite directions and by the same magnitude.)

The delay-coupled two-laser system can be modelled by rate equations for the

**Table 1.** Parameters of the model and their values

Symbol	Meaning	Value
$\alpha$	Linewidth enhancement factor	2.0
$\kappa$	Coupling rate	0.047
$T$	Decay constant	150
$\Gamma_{el}$	Electron decay rate	$150 \times 10^9 \text{ s}^{-1}$
$\Gamma_{ph}$	Photon decay rate	$1 \times 10^9 \text{ s}^{-1}$
$\xi$	Differential gain	$790 \text{ s}^{-1}$
$J_{thr}$	Threshold current density	$1 \times 10^{18} \text{ s}^{-1}$

complex-valued slowly varying envelopes of the optical fields  $E_{1,2}(t)$  and the real valued inversions  $N_{1,2}(t)$  of the lasers; see, for example, Ref. [39]. In dimensionless form the model equations can be written as

$$\dot{E}_1(t) = (1 + i\alpha)N_1(t)E_1(t) + \kappa e^{-iC_p}E_2(t - \tau) + i\frac{\nu_1}{2\pi}E_1(t), \quad (1)$$

$$T\dot{N}_1(t) = \frac{\xi}{2\Gamma_{ph}\Gamma_{el}}(J - J_{thr}) - N_1(t) - (1 + 2N_1(t))|E_1(t)|^2, \quad (2)$$

$$\dot{E}_2(t) = (1 + i\alpha)N_2(t)E_2(t) + \kappa e^{-iC_p}E_1(t - \tau) + i\frac{\nu_2}{2\pi}E_2(t), \quad (3)$$

$$T\dot{N}_2(t) = \frac{\xi}{2\Gamma_{ph}\Gamma_{el}}(J - J_{thr}) - N_2(t) - (1 + 2N_2(t))|E_2(t)|^2, \quad (4)$$

where time  $t$  is in units the photon decay time. Equations (1)–(4) are delay differential equations (DDEs), where the time delay  $\tau$  accounts for the propagation time of the light between the two spatially separated lasers. The lasers are characterised by (equal) values of the linewidth enhancement factor  $\alpha$ , the electron decay rate  $\Gamma_{el}$ , the photon decay rate  $\Gamma_{ph}$ , the differential gain  $\xi$ , the ratio  $T = \frac{\Gamma_{el}}{\Gamma_{ph}}$ , and current density at threshold  $J_{thr}$ . The coupling terms are symmetrical and contain the coupling rate  $\kappa$ , while  $C_p$  controls the phase relationship between the two electric fields. Note that  $C_p$  can be adjusted by sub-wavelength changes of the distance between the two lasers [21]; in this study we choose  $C_p = 0$  throughout. The detuning between the two lasers enters in the last term of (1) and (3) via the optical frequencies  $\nu_{1,2}$  of lasers 1 and 2, respectively. Numerical values of the parameters are chosen to match the experimental conditions; they can be found in Table 1.

Linear stability analysis of the solitary laser model, *i.e.*, in the absence of coupling ( $\kappa = 0$ ), reveals two states of the laser as equilibria of Eqs. (1)–(4): the off-state,  $(|E_s|^2, N_s) = (0, \frac{\xi}{2\Gamma_{el}\Gamma_{ph}}(J - J_{thr}))$ , and the on-state  $(|E_s|^2, N_s) = (\frac{\xi}{2\Gamma_{el}\Gamma_{ph}}(J - J_{thr}), 0)$ . Below threshold ( $J < J_{thr}$ ) the on-state is unstable and the off-state is stable. At the threshold  $J = J_{thr}$  the two states interchange stability, so that the on-state becomes stable and the off-state unstable. This is associated with the onset of the laser oscillation. Furthermore, above threshold ( $J > J_{thr}$ ) we find damped intensity oscillations as response to perturbations from the equilibrium state. These characteristic oscillations are known as the relaxation oscillations. The relaxation oscillation frequency in GHz is

given by

$$\nu_{RO} = \frac{1}{2\pi} \sqrt{\xi(J - J_{thr})} \quad (5)$$

and it defines a characteristic time scale of the lasers. Already quite small external influences, such as feedback or coupling, can destabilise the laser by undamping the relaxation oscillations.

The simplest non-trivial solutions of Eqs. (1)–(4) in the presence of coupling ( $\kappa > 0$ ), known as compound laser modes (CLMs), are given as

$$(E_1(t), E_2(t), N_1(t), N_2(t)) = (R_1^s e^{i\omega^s t}, R_2^s e^{i\omega^s t + i\phi}, N_1^s, N_2^s) \quad (6)$$

for given fixed values  $R_{1,2}$ ,  $N_{1,2}$ ,  $\omega^s$  and  $\phi$ . CLMs describe continuous wave emission (cw) of the coupled laser system, where the optical fields oscillate with the joint frequency  $\omega^s$ , while the intensities and inversions of the two lasers are constant in time, that is,  $(|E_{1,2}(t)|^2, N_{1,2}(t)) = ((R_{1,2}^s)^2, N_{1,2}^s)$ . Hence, operation at a CLM corresponds to locking between the two lasers. To find the CLMs one needs to solve six coupled transcendental equations, which is best done with numerical continuation techniques; this has the advantage that the stability of the CLM and their bifurcations can be determined as well [11].

In this paper we are interested in bifurcations of CLMs that give rise to dynamics associated with the relaxation oscillation frequency and the detuning frequency. We proceed by providing experimental evidence for different types of dynamics, which are then explained via bifurcation scenarios. Throughout, we use for ease of comparison the detuning  $\Delta$  (via the frequency  $\nu_2$  of laser 2) and the identical pump current  $J$  (presented in units of the threshold current  $J_{thr}$ ) as the bifurcation parameters.

### 3. Characterisation of the dynamics

Figure 2 shows experimental measurements of the dynamics of the coupled laser system for increasing detuning  $\Delta$  for three different pump currents of the laser, 27 mA (a), 20 mA (b), and 17 mA (c). Panels (a1), (b1), and (c1) show the peak wavelength of the optical spectrum of both lasers for the different pump currents, respectively. For small detuning, on the order  $|\Delta| \leq 5$  GHz, it can be seen that the wavelengths of both lasers coincide. This defines the locking region, where the two lasers operate at the same optical frequency and have constant intensities; recall that these are the defining characteristics of the CLMs given by Eq. (6). As a function of the detuning, the optical frequency features a characteristic step-like behaviour. This was reported in Ref. [12], where the step-like structure was attributed to saddle-node bifurcations of the CLMs. The locking boundary in figure 2 is indicated by the dashed lines; its width is almost constant for the three different pump currents. Panels (a2), (b2), and (c2) show the peaks of the rf spectrum of laser 1. Importantly, inside the locking region one may also find dynamical instabilities (even though the two lasers remain locked at the same frequency). For high pump currents, as in Fig. 2(a1), one can identify relaxation oscillations (ROs) of the

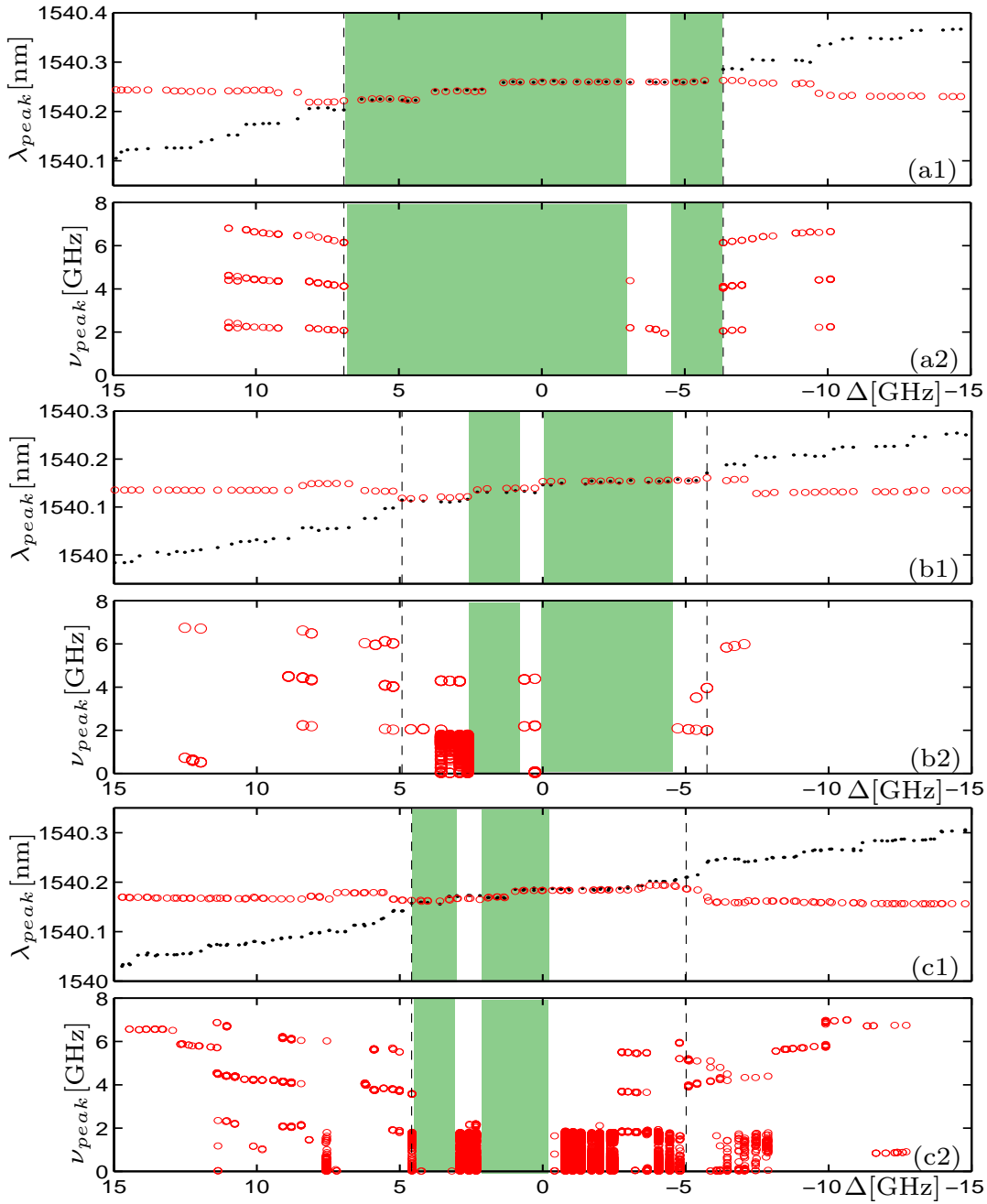


**Figure 2.** Experimental bifurcation diagrams for increasing  $\Delta$  and the currents 27 mA (a), 21 mA (b), and 17 mA (c). Shown in panel (a1) (b1), and (c1) are the wavelength of the main peaks of the optical spectra of laser 1 (circles) and laser 2 (dots); shown in panels (a2), (b2), and (c2) are the main peaks of the rf spectra (defined as at least 1.2 dB above the noise level). The dashed lines indicate the locking region where both lasers emit at the same optical frequency; the shaded regions indicate intervals of stable cw-emission of the coupled laser system.

two lasers with a single frequency in the rf spectrum and possible higher harmonics. For lower pump current, as in Fig. 2(b1), complicated dynamics can be found also around



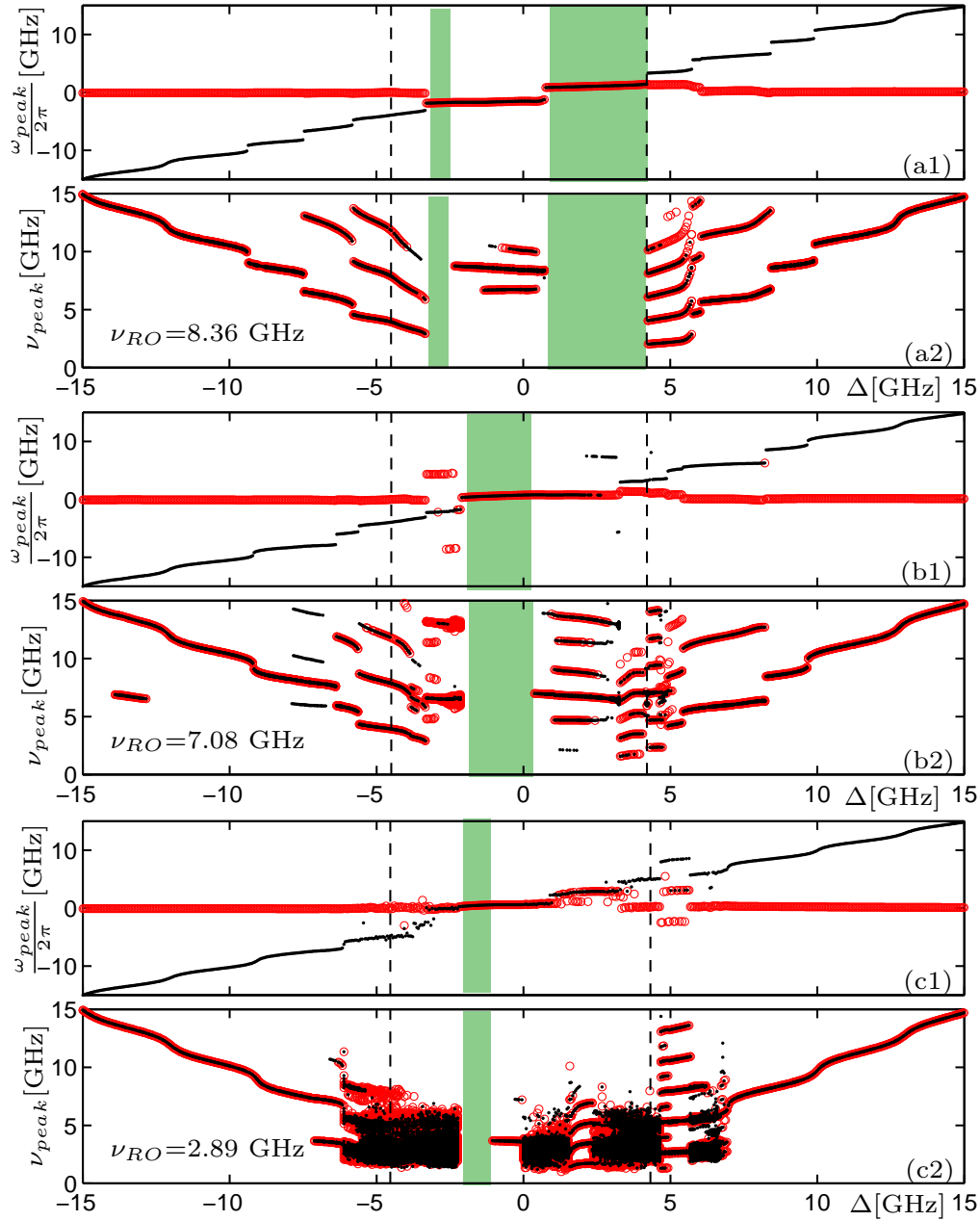


**Figure 3.** Bifurcation diagram for increasing  $\Delta$  obtained by numerical simulations of Eqs. (1)–(4) for the pump currents  $J = 4.6J_{thr}$  (a),  $J = 4J_{thr}$  (b), and  $J = 1.38J_{thr}$  (c). Shown in panel (a1) (b1), and (c1) is the wavelength of the main peaks of the optical spectra of laser 1 (grey dots) and laser 2 (black dots); shown in panels (a2), (b2), and (c2) are peaks of the rf spectra that are at least 1.2 dB above the experimental noise level. The dashed lines indicate the width of the locking region, as given by the outer-most saddle-node bifurcation of CLMs; the shaded regions indicate intervals of stable cw-emission of the coupled lasers system.

$\Delta = 1$  GHz; they are characterised by broadened peaks in the low-frequency part of the rf spectrum. These regions of complicated dynamics become larger for lower pump

current, as is shown in figure 2(c1).

For large detuning, and any value of the pump current in figure 2, the optical frequencies of the two lasers are not identical anymore. Hence, the coupled system operates outside its locking region, and both lasers operate close to their solitary laser frequency. The frequency of the undetuned laser 1 stays almost constant, whereas the frequency of the detuned laser 2 changes in accordance with the detuning  $\Delta$ , but in characteristic steps. The rf spectra of the lasers show intensity oscillations with a frequency that corresponds to the difference between the two laser frequencies. We refer to this type of periodic dynamics as detuning oscillations (DOs).

Figure 3 shows the dynamics as found by numerical simulation of the compound laser model Eqs. (1)–(4) for increasing  $\Delta$  for three pump currents,  $J = 4.6J_{thr}$  (a),  $J = 4J_{thr}$  (b), and  $J = 1.38J_{thr}$  (c). The agreement with the experimental results in figure 2 is so good that the different dynamical regimes can be identified clearly. There is the locking region around zero detuning, where the lasers operate at the same frequency. As in the experiment, we find cw-emission (stable locking) and relaxation oscillation (ROs) inside the locking region. Furthermore, we again find detuning oscillations in the region of large detuning. The boundary of the frequency locking region was identified in Ref. [12] as a saddle-node bifurcation of a CLM; the dashed lines in the individual panels of figure 3 give the location of these saddle-node bifurcations and, hence, the locking boundary.

Overall it can be seen that the dynamics becomes more complicated when the lasers are operated closer to their laser threshold. Furthermore, the rf spectra show that the frequency of ROs remains practically unchanged as the detuning  $\Delta$  changes; this is to be expected since the RO frequency scales with the pump current. For large detuning, on the other hand, the DOs indeed depend on the detuning  $\Delta$ . For very large detuning this dependence is approximately linear, but as the detuning approaches the locking region a typical stair-like structure emerges, which gives rise to hysteresis loops of DOs (not shown) when the detuning is swept up and down; see Ref. [55].

## 4. Bifurcation analysis

In order to get a comprehensive and consistent picture of the dynamics of the coupled laser system we now present a bifurcation analysis of the model equations (1)–(4) with the tool of numerical continuation; specifically we use the packages DDE-BIFTOOL [9] and PDDE-CONT [51]. As was already mentioned, our main bifurcation parameters are the detuning  $\Delta$  and the pump current  $J$ .

### 4.1. Locking region

We start with the stability analysis of the compound laser modes from Eq. (6). They are the basic states of the coupled laser system and form the underlying structure for all other dynamical instabilities. Specifically, bifurcations of CLMs reveal the structure

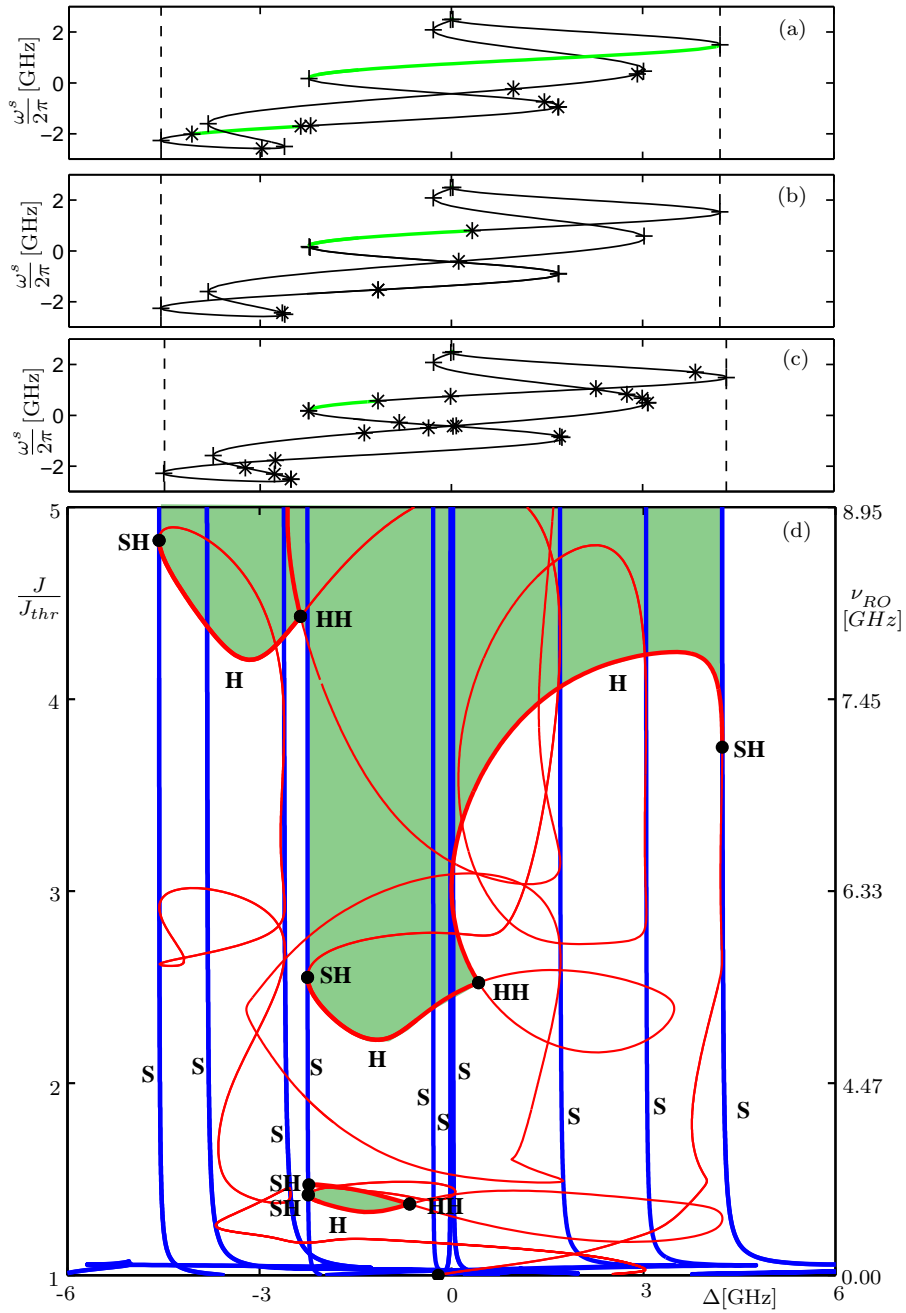


**Figure 4.** The locking region of Eqs. (1)–(4). Shown are one-parameter bifurcation diagrams in the  $(\Delta; \omega^s)$ -projection for the pump currents  $J = 4.6J_{thr}$  (a),  $J = 4J_{thr}$  (b),  $J = 1.38J_{thr}$  (c); stable CLMs are green, plusses (+) indicate saddle-node bifurcations and stars (\*) Hopf bifurcations. Panel (d) shows the two-parameter bifurcation diagram in the  $(\Delta; J)$ -plane, consisting of curves of saddle-node (S) and Hopf (H) bifurcations of CLMs, which meet at saddle-node Hopf (SH) and double Hopf (HH) points. The CLMs are stable in the green shaded region; the scale on the right shows the relaxation oscillation frequency of the solitary lasers.

and the dynamics within the locking region.

Figure 4 illustrates the CLM structure near the locking region. Shown in panels (a)–(c) are one-parameter bifurcation diagrams for three different values of the pump current  $J$ , while panel (d) is the two-parameter bifurcation diagram of CLMs near the locking region in the  $(\Delta; J)$ -plane. The width of the locking region is given by the two outer-most saddle-node bifurcation curves in figure 4(d); note that this width is practically constant as a function of  $J$ , and only changes close to the laser threshold; see Ref. [10] for a detailed study of the bifurcation structure of the CLMs close to the laser threshold. The CLMs branches in figure 4(a)–(c) for the pump currents,  $J = 4.6J_{thr}$ ,  $J = 4J_{thr}$  and  $J = 1.38J_{thr}$ , exist inside the dashed lines, marking the outer-most saddle-node bifurcations. While the lasers are frequency locked inside the locking region, this does not mean that the CLMs are necessarily stable. Their stability is gained or lost in saddle-node bifurcations (+) or Hopf bifurcations (\*), and stable CLM branches appear green in panels (a)–(c). Recall that a stable CLM corresponds to stable locking, meaning that the lasers produce constant intensity output at the same frequency. As  $J$  decreases, the width of the locking stays almost constant – however the stability and the dynamics within the locking region changes. In particular, Hopf bifurcations mark the onset of ROs within the locking region.

Figure 4(a)–(c) correspond to horizontal cross sections of the two-parameter bifurcation diagram in the  $(\Delta; J)$ -plane in figure 4(d). Shown are curves of saddle-node bifurcations (blue), Hopf bifurcation (red), which divide the  $(\Delta; J)$ -plane into regions of different behaviour. Of immediate interest is the green region of stable CLMs, that is, of full locking. For high values of the pump current  $J$  stable CLMs exist within the whole locking region. However, comparison with panel (a) shows that there are different stable CLMs, with different values of the frequency  $\omega^s$ . The system jumps from one of these stable CLMs to another, which explains the step-like nature of the optical frequency observed in figure 2; see also Ref. [12], where the stability of the CLMs for high pump currents is studied experimentally and theoretically. For lower pump current  $J$  the stable CLM region becomes narrower, *i.e.*, the detuning interval where stable CLMs can be observed becomes smaller. Eventually, around  $J \leq 2J_{thr}$  there are no stable CLMs at all. Notice the small isolated CLM stability region around  $J = 1.5J_{thr}$ . Overall, the boundaries of the region(s) of stable CLMs in figure 4(d) are formed by different parts of saddle-node and Hopf bifurcation curves, which meet at several special points, namely saddle-node Hopf (SH) points and double Hopf (HH) points. These are codimension-two bifurcation points that act as organising centres for dynamical systems, specifically marking the change from one type of boundary of the stable CLM region to another. Moreover, these codimension-two bifurcation points indicate that there is a more complex bifurcation structure including bifurcations of periodic orbits [33].

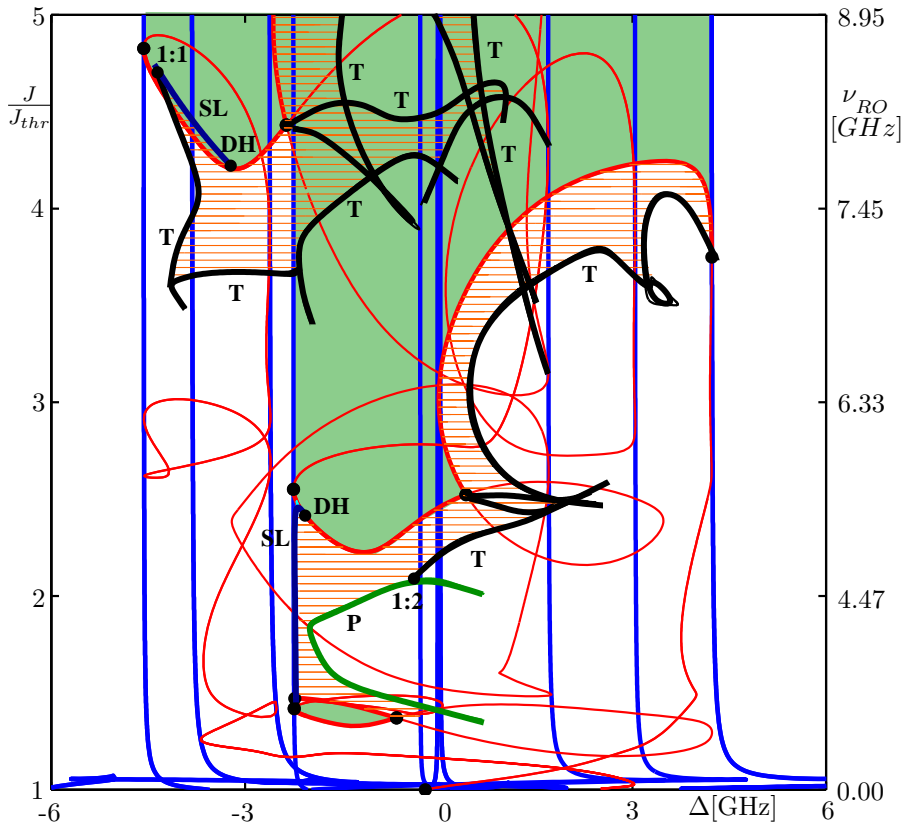


**Figure 5.** Two-parameter bifurcation diagram in the  $(\Delta; J)$ -plane showing also regions (hatched) of stable relaxation oscillations; compare with Fig 4. RO stability regions are bounded by curves of saddle-node of limit cycles (SL) bifurcations, period doubling (P) and torus (T) bifurcations. These bifurcation curves of ROs may meet at degenerate Hopf (DH), 1:1 resonance, and 1:2 resonance points.

#### 4.2. Stable relaxation oscillations

We now consider the stable periodic orbits that bifurcate at the different curves of Hopf bifurcations bounding the stable CLM regions. They turn out to be the typical relaxation oscillations whose frequency, given by Eq. (5), depends mainly on the pump current  $J$ . Figure 5 shows the RO stability regions (red hatching) in the  $(\Delta; J)$ -projection. Indeed all regions of stable ROs are inside the locking region, which agrees with the results in figure 2 and figure 3. The ROs were continued for fixed  $J$  and varying  $\Delta$ , and this showed that their frequency remains practically constant with  $\Delta$ ; compare with figure 2. Relaxation oscillations that are born in Hopf bifurcations of CLMs can be identified in figure 2 by a peak in the rf spectrum that lies inside the locking region.

There are further bifurcations of ROs where their stability is lost, including saddle-node bifurcations of limit cycles (SL) bifurcations, period-doubling (P) bifurcations, and torus (T) bifurcations; note that we only show those branches that actually bound unstable RO regions. Figure 5 also shows that there is multistability in the system:

different ROs and CLMs may be stable simultaneously. This is due to the fact that the locking region contains several CLMs, each of which can undergo a Hopf bifurcation to ROs. Specifically, for high pump current  $J$ , ROs bifurcate from Hopf bifurcations of CLMs and their stability regions overlap with other stable CLMs. Thus, hysteresis effects are to be expected when parameters are changed.

#### 4.3. Stable detuning oscillations

Outside the locking region stable detuning oscillations dominate the dynamics. Figure 6 shows branches of DOs for different values of the pump current,  $J = 4.6J_{thr}$  (a),  $J = 4J_{thr}$  (b), and  $J = 1.38J_{thr}$  (c), whereas the stability region of the DOs in the  $(\Delta; J)$ -plane (d). From panels (a)–(c) it can be seen that the frequency  $\nu_{DO}$  of the DOs scales with the detuning  $\Delta$ . Furthermore, for all values of  $J$  the frequency  $\nu_{DO}$  of the DOs approaches the detuning  $\Delta$ . This agrees with the experimental observation outside the locking region in Fig. 2; see also the findings for high pump currents in Refs. [12, 55]. When approaching the locking region the DOs undergo a sequence of saddle-node of limit cycle bifurcations in which they destabilise and then restabilise. Each saddle-node bifurcations of limit cycles is associated with a jump in the frequency  $\nu_{DO}$  of the DOs. As observed in figure 2, this jump is on the order of the external round-trip frequency. Eventually, for sufficiently high  $J$  the branch of DOs ends at a homoclinic bifurcation; here the period of the DOs goes to infinity and, thus, the frequency goes to zero. In this homoclinic connection the periodic orbit corresponding to the DO ‘hits’ an unstable CLM. Figure 6(d) shows the complete stability region of DOs (yellow hatching); notice the curves SL that are responsible for the steps in panels (a) and (b), where the dynamics is dominated by stable locking, ROs, and DOs. On the other hand, for pump currents below  $2.5J_{thr}$  much more complicated behaviour is to be expected; compare with figure 2(c) and figure 3(c).

Finally, figure 7 shows evidence of a homoclinic bifurcation; specifically, an example of a periodic orbit very close to a homoclinic bifurcation. Panel (a) shows the time series of the intensity of laser 1 and laser 2, and panel (b) the projection onto  $(\text{Im}[E]; \text{Re}[E]; N)$ -space. The trajectory stays for a long time in the vicinity on an unstable CLM (the grey circles). It then drifts away along the unstable manifold of the CLM, which leads to a large excursion into phase space. Eventually the trajectory spirals back towards the unstable CLM, by following its stable manifold. This involves oscillations on the RO time scale.

#### 4.4. Overall bifurcation diagram

The dynamical complexity of the two mutually delay-coupled semiconductor lasers can be summarised best by assembling the stability regions of CLMs, ROs and DOs with the associated bifurcation curves into a single bifurcation diagram, as is shown in figure 6. This image can be understood as an ‘explorer’s map’ to the dynamics of this delay-coupled laser system. In particular, this representation brings out the different kinds of

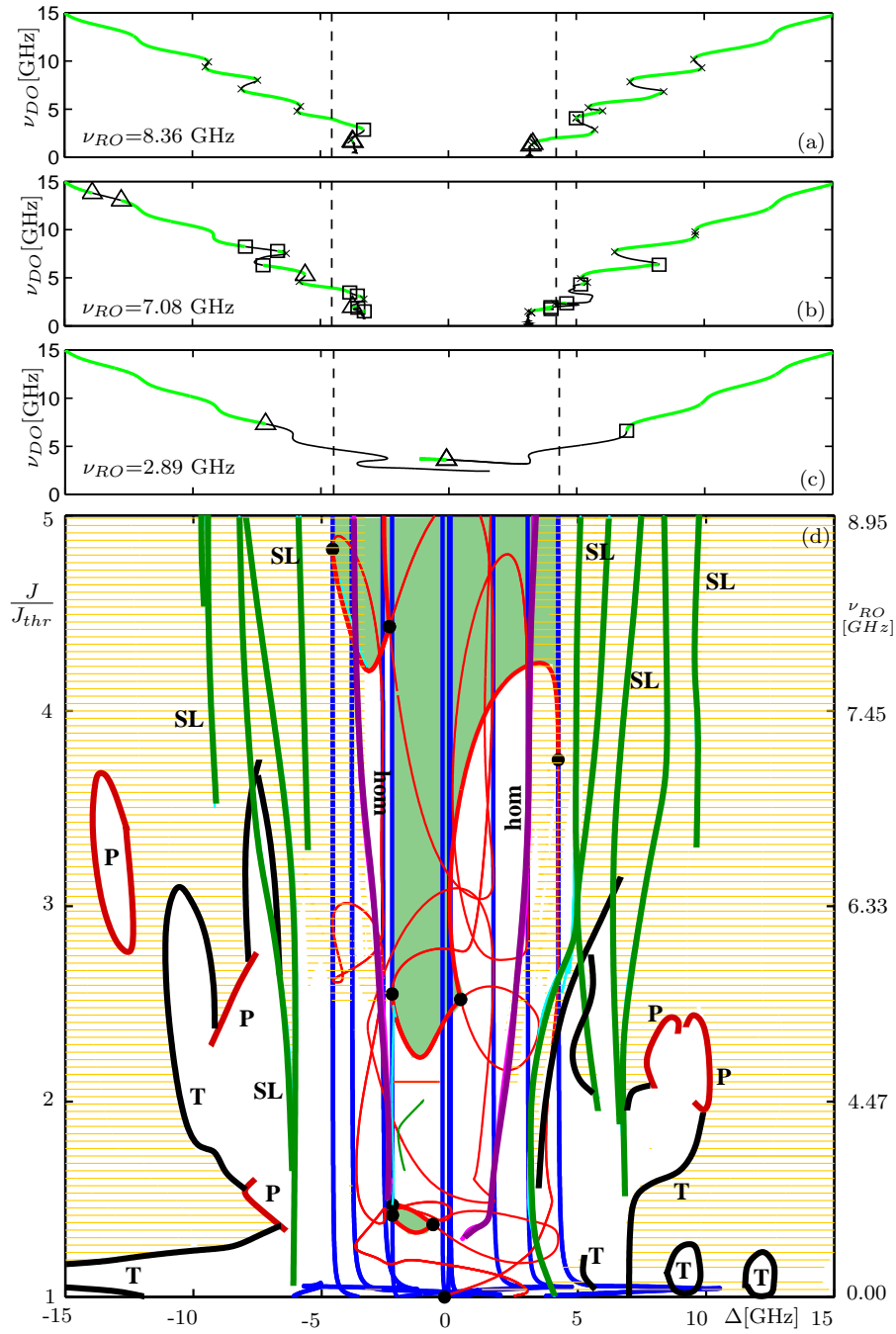


**Figure 6.** Stability region of detuning oscillations of Eqs. (1)–(4). Shown are one-parameter bifurcation diagrams in the  $(\Delta; \nu_{DO})$ -projection for the pump currents  $J = 4.6J_{thr}$  (a),  $J = 4J_{thr}$  (b),  $J = 1.38J_{thr}$  (c); stable DOs are green, crosses (×) indicate saddle-node of limit cycle bifurcations, squares (□) torus bifurcations, and triangles (△) period doublings. Panel (d) shows the DO stability region (yellow hatching) in the  $(\Delta; J)$ -plane.

multistabilities as overlapping CLM, RO and DO stability regions. The white region in figure 6 corresponds to even more complicated, and possibly chaotic dynamics. It can

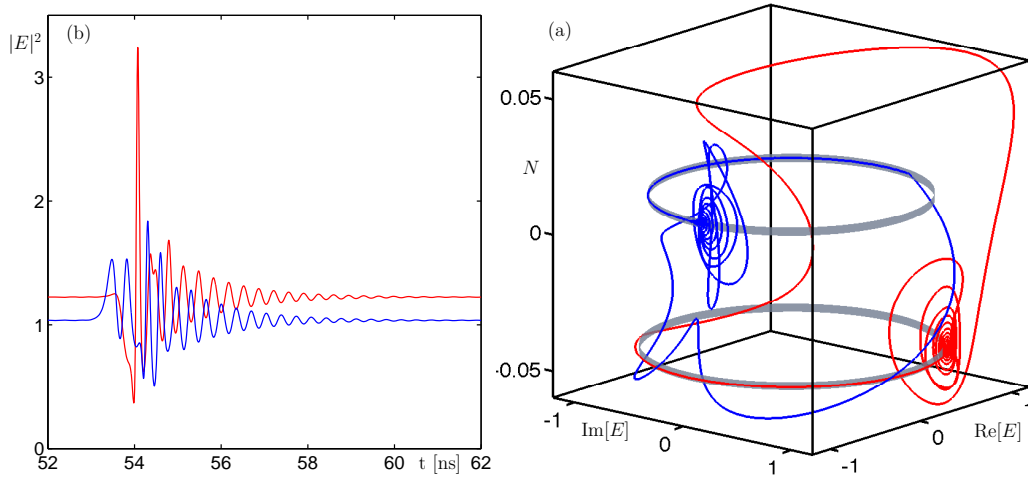


**Figure 7.** Periodic orbit close to a homoclinic bifurcation for  $(\Delta; J) \approx (1.5\text{GHz}; 1.41J_{thr})$  (where  $\nu_{RO} \approx 2.89\text{GHz}$ ). Shown are the time series of the intensities of laser 1 (red) and laser 2 (blue) over one period (a), and the corresponding periodic trajectories in  $(\text{Im}[E]; \text{Re}[E]; N)$ -space (b). The grey circles in panel (b) are CLMs that are closely followed by parts of the trajectories of laser 1 and laser 2, respectively.

be entered via torus and period doubling bifurcations, which hints already at two classic routes to chaos.

## 5. Conclusions and outlook

We presented a comprehensive study of the dynamics of two mutually delay-coupled semiconductor lasers, where we focused on the influence of the detuning between the two lasers for different values of the pump current. Experiments show a qualitatively different behaviour for low as opposed to high pump current, and this has been confirmed by the bifurcation analysis of the rate equation model.

Our study provides important insight into the dynamical complexity of delay-coupled oscillators. Namely, since the individual lasers are stable, all dynamics we found arises due to coupling-induced instabilities. We identified three different relevant time scales of the system: (i) the intrinsic relaxation oscillation frequency of the individual oscillators; (ii) the detuning oscillation frequency, which is due to the coupling and characterises the frequency difference between the individual oscillators; and (iii) the external round-trip frequency associated with the delay-time. The overall dynamics of the system arises from the interplay between oscillations associated with these different time scales.

Generally, delay in the coupling leads to locking with multiple frequencies. In the delay-coupled laser system this is expressed by multiple compound laser modes with



different frequencies, which are created and destroyed in saddle-node bifurcations; see also Refs. [12, 48, 56]. Because the different CLMs may undergo Hopf bifurcations, we find several regions of stable relaxation oscillations. For large detuning, on the other hand, the dynamics of the coupled system is dominated by the detuning frequency, which goes to zero as the locking region is approached [1]. However, due to the presence of the delay, we find frequency jumps on the order of the external round-trip frequency; see also Ref [55]. Bifurcation analysis of the coupled laser system reveals that this ‘frequency discretisation’ is associated with saddle-node bifurcations of periodic orbits.

We identified the locking regions (frequency locking and stable locking), and the stability regions of relaxation and detuning oscillations and assembled them into a two-parameter bifurcation diagram in the plane of detuning versus pump current. The overall conclusion is that for sufficiently high pump current only stable compound laser modes, relaxation oscillations, and detuning oscillations can be found. For low pump currents, below two times the threshold current, on the other hand, complicated dynamics and chaos may be observed. Their detailed study remains an interesting subject for further investigation.

## Acknowledgements

The authors would like to thank W. Elsässer and M. Peil for their support in the experimental realisation of the system, and Nortel Networks for providing the excellent DFB lasers.

## References

- [1] R. Adler. A study of locking phenomena in oscillators. *Proc. IRE*, 34:351–357, 1946. neu abgedruckt in *Proc. IEEE* 61, (1973), 1380–1385.
- [2] A. Argyris, D. Syvridis, L. Larger, V. Annovazzi-Lodi, P. Colet, I. Fischer, J. García-Ojalvo, C. R. Mirasso, L. Pesquera, and K. A. Shore. Chaos-based communications at high bit rates using commercial fibre-optic links. *Nature*, 438(7066):343–346, November 2005.
- [3] D.A.W. Barton, B. Krauskopf, and R.E. Wilson. Collocation schemes for periodic solutions of neutral delay differential equations. *Journal of Difference Equations and Applications*, 12(11):1087–1101, 2006.
- [4] R.F. Broom, E. Mohn, C. Risch, and R. Salathe. Microwave self-modulation of a diode laser coupled to an external cavity. *IEEE J. Quantum Electr.*, QE-6:328, 1970.
- [5] J. M. Buldú, J. García-Ojalvo, and M. C. Torrent. Delay-induced resonances in an optical system with feedback. *Phys. Rev. E*, 69(4):046207, Apr 2004.
- [6] C.-U. Choe, V. Flunkert, P. Hövel, H. Benner, and E. Schöll. Conversion of stability in systems close to a hopf bifurcation by time-delayed coupling. *Physical Review E (Statistical, Nonlinear, and Soft Matter Physics)*, 75(4):046206, 2007.
- [7] Guy Van der Sande, Miguel C. Soriano, Ingo Fischer, and Claudio R. Mirasso. Dynamics, correlation scaling, and synchronization behavior in rings of delay-coupled oscillators. *Physical Review E (Statistical, Nonlinear, and Soft Matter Physics)*, 77(5):055202, 2008.
- [8] O. Diekmann, S. A. Van Gils, and S. M. Verduyn Lunel. *Delay Equations: Functional-, Complex-, and Nonlinear Analysis*. Springer Verlag, New York, 1995.

- [9] K. Engelborghs, T. Luzyanina, and G. Samaey. DDE-BIFTOOL v. 2.00 user manual: a matlab package for bifurcation analysis of delay differential equations. Technical Report TW-330, Department of Computer Science, K. U. Leuven, Leuven, oct 2001.
- [10] H. Erzgräber, B. Krauskopf, and D. Lenstra. Mode structure of delay-coupled semiconductor lasers: influence of the pump current. *Journal of Optics B: Quantum and Semiclassical Optics*, 7(11):361–371, 2005.
- [11] H. Erzgräber, B. Krauskopf, and D. Lenstra. Coupled laser modes of mutually delay-coupled lasers. *SIAM J. Appl. Dyn. Syst.*, 5(1):30–65, 2006.
- [12] H. Erzgräber, D. Lenstra, B. Krauskopf, E. Wille, M. Peil, I. Fischer, and W. Elsässer. Mutually delay-coupled semiconductor lasers: Mode bifurcation scenarios. *Opt. Commun.*, 255(4-6):286–296, 2005.
- [13] I. Fischer, T. Heil, and W. Elsässer. Emission dynamics of semiconductor lasers subject to delayed optical feedback: an experimentalist’s perspective. In B. Krauskopf and D. Lenstra, editors, *Fundamental Issues of Nonlinear Laser Dynamics*, volume 548 of *AIP Conference Proceedings*, pages 66–86, New York, 2000.
- [14] I. Fischer, O. Hess, W. Elsässer, and E. Göbel. High-dimensional chaotic dynamics of an external cavity semiconductor laser. *Phys. Rev. Lett.*, 73:2188–2191, 1994.
- [15] I. Fischer, G. H. M. van Tartwijk, A. M. Levine, W. Elsässer, E. Göbel, and D. Lenstra. Fast pulsing and chaotic itinerancy with a drift in the coherence collapse of semiconductor lasers. *Phys. Rev. Lett.*, 76:220–223, 1996.
- [16] H. Fujino and J. Ohtsubo. Synchronization of chaotic oscillations in mutually coupled semiconductor lasers. *Opt. Rev.*, 8:351–357, 2001.
- [17] J. García-Ojalvo and Rajarshi Roy. Spatiotemporal communication with synchronized optical chaos. *Phys. Rev. Lett.*, 86(22):5204–5207, May 2001.
- [18] K. Green, B. Krauskopf, and K. Engelborghs. One-dimensional unstable eigenfunction and manifold computations in delay differential equations. *J. Computational Physics*, 197(1):86–98, 2004.
- [19] J. Guckenheimer and P. Holmes. *Nonlinear Oscillations, Dynamical Systems, and Bifurcations of Vector Fields*. Springer-Verlag, New York, 1986.
- [20] J. K. Hale and S. M. Verduyn Lunel. *Introduction to Functional Differential Equations*. Springer Verlag, New York, 1993.
- [21] T. Heil, I. Fischer, W. Elsässer, and A. Gavrielides. Dynamics of semiconductor lasers subject to delayed optical feedback: The short cavity regime. *Phys. Rev. Lett.*, 87:243901, 2001.
- [22] T. Heil, I. Fischer, W. Elsässer, B. Krauskopf, K. Green, and A. Gavrielides. Delay dynamics of semiconductor lasers with short external cavities: Bifurcation scenarios and mechanisms. *Phys. Rev. E*, 67:066214, 2003.
- [23] T. Heil, I. Fischer, W. Elsässer, J. Mulet, and C. R. Mirasso. Chaos synchronization and spontaneous symmetry-breaking in symmetrically delay-coupled semiconductor lasers. *Phys. Rev. Lett.*, 86:795–798, 2001.
- [24] C. H. Henry. Theory of the phase noise and power spectrum of a single mode injection laser. *IEEE J. Quantum Electron.*, 19:1391–1397, 1983.
- [25] A. Hohl, A. Gavrielides, T. Erneux, and V. Kovanis. Localized synchronization in two coupled nonidentical semiconductor lasers. *Phys. Rev. Lett.*, 78:4745–4748, 1997.
- [26] A. Hohl, A. Gavrielides, T. Erneux, and V. Kovanis. Quasiperiodic synchronization for two delay-coupled semiconductor lasers. *Phys. Rev. A*, 59:3941–3949, 1999.
- [27] J. Javaloyes, P. Mandel, and D. Pieroux. Dynamical properties of lasers coupled face to face. *Phys. Rev. E*, 67:036201, 2003.
- [28] D.M. Kane and K.A. Shore (Eds.). *Unlocking Dynamical Diversity: Optical Feedback Effects on Semiconductor Lasers*. Wiley, 2005.
- [29] S. Kim, S.H. Park, and C.S. Ryu. Multistability in coupled oscillator systems with time delay. *Phys. Rev. Lett.*, 79:2911–2914, 1997.

- [30] B. Krauskopf. Bifurcation analysis of lasers with delay. In D.M. Kane and K.A. Shore, editors, *Unlocking Dynamical Diversity: Optical Feedback Effects on Semiconductor Lasers*, pages 147–183, New York, 2005. Wiley.
- [31] B. Krauskopf and K. Green. Computing unstable manifolds of periodic orbits in delay differential equations. *J. Computational Physics*, 186(1):230–249, 2003.
- [32] B. Krauskopf and D. Lenstra, editors. *Fundamental Issues of Nonlinear Laser Dynamics*, volume 548 of *AIP Conference Proceedings*. American Institute of Physics, 2000.
- [33] Yu.A. Kuznetsov. *Elements of Applied Bifurcation Theory*. Springer-Verlag, New York, 1995.
- [34] R. Lang and K. Kobayashi. External optical feedback effects on semiconductor injection laser properties. *IEEE J. Quantum Electron.*, QE-16:347–355, 1980.
- [35] D. Lenstra, B. H. Verbeek, and A. J. den Boef. Coherence collapse in single-mode semiconductor lasers due to optical feedback. *QE-21*, page 674, 1985.
- [36] S.M. Verduyn Lunel and B. Krauskopf. The mathematics of delay equations with an application to the Lang-Kobayashi equations. In B. Krauskopf and D. Lenstra, editors, *Fundamental Issues of Nonlinear Laser Dynamics*, volume 548 of *AIP Conference Proceedings*, pages 66–86, New York, 2000.
- [37] N. Minorsky. *Nonlinear Oscillations*. D. Van Nostrand, 1962.
- [38] J. Mørk, J. Mark, and B. Tromborg. Route to chaos and competition between relaxation oscillations for a semiconductor laser with optical feedback. *Phys. Rev. Lett.*, 65:1999–2002, 1990.
- [39] J. Mulet, C. Masoller, and C. R. Mirasso. Modeling bidirectionally coupled single-mode semiconductor lasers. *Phys. Rev. A*, 65:063815, 2002.
- [40] J. Mulet, C. Mirasso, T. Heil, and I. Fischer. Synchronization scenario of two distant mutually coupled semiconductor lasers. *J. Opt. B: Quantum Semiclass. Opt.*, 6:97–105, 2004.
- [41] E. Niebur, H.G. Schuster, and D.M. Kammen. Collective frequencies and metastability in networks of limit-cycle oscillators with time delay. *Phys. Rev. Lett.*, 67(20):2753–2756, Nov 1991.
- [42] H. Olesen, J.H. Osmundsen, and B. Tromborg. Nonlinear dynamics and spectral behavior for an external cavity semiconductor laser. *QE-22*, page 762, 1986.
- [43] M. Peil, T. Heil, I. Fischer, and W. Elsässer. Synchronization of chaotic semiconductor laser systems: A vectorial coupling-dependent scenario. *Phys. Rev. Lett.*, 88:174101, 2002.
- [44] D. Pieroux and P. Mandel. Low-frequency fluctuations in the Lang-Kobayashi equations. *Phys. Rev. E*, 68:036204, 2003.
- [45] D. V. Ramana Reddy, A. Sen, and G. L. Johnston. Time delay induced death in coupled limit cycle oscillators. *Phys. Rev. Lett.*, 80:5109–5112, 1998.
- [46] T. Sano. Antimode-dynamics and chaotic itinerancy in the coherence collapse of semiconductor lasers with optical feedback. *Phys. Rev. A*, 50:2719–2726, 1994.
- [47] E. Schöll and H. G. Schust, editors. *Handbook of Chaos Control (2nd edition)*, Schöll, E. and Schuster, H. G. (Eds.), chapter W. Just, On global properties of time-delayed feedback control, pages 85–108. Wiley-VCH, Weinheim, 2006.
- [48] H.G. Schuster and P. Wagner. Mutual entrainment of two limit cycle oscillators with time delayed coupling. *Progr. Theor. Phys.*, 81:939–945, 1989.
- [49] Gautam C. Sethia, Abhijit Sen, and Fatihcan M. Atay. Clustered chimera states in delay-coupled oscillator systems. *Physical Review Letters*, 100(14):144102, 2008.
- [50] S. H. Strogatz. *Sync: The Emerging Science of Spontaneous Order*. Hyperion, 2003.
- [51] R. Szalai. PDDE-CONT: A continuation and bifurcation software for delay-differential equations. Technical report, Budapest, Hungary, 2005.
- [52] A. Uchida, Rogister F., J. García-Ojalvo, and R. Roy. Synchronization and communication with chaotic laser systems. *Progress in Optics*, 48:203–341, 2005.
- [53] G. D. VanWiggen and R. Roy. Communication with chaotic lasers. *Science*, 279:1198–1200, 1998.
- [54] S.M. Wiczorek, B. Krauskopf, T.B. Simpson, and D. Lenstra. The dynamical complexity of

- optically injected semiconductor lasers. *Physics Reports*, 416(1-2):1–128, 2005.
- [55] H.-J. Wünsche, S. Bauer, J. Kreissl, O. Ushakov, N. Korneyev, F. Henneberger, E. Wille, H. Erzgräber, M. Peil, W. Elsässer, and I. Fischer. Synchronization of delay-coupled oscillators: A study on semiconductor lasers. *Phys. Rev. Lett.*, 94:163901, 2005.
- [56] S. Yanchuk. Discretization of frequencies in delay coupled oscillators. *Physical Review E (Statistical, Nonlinear, and Soft Matter Physics)*, 72(3):036205, 2005.